THE JOURNAL OF BIOLOGICAL CHEMISTRY
Vol. 278, No. 17, Issue of April 25, pp. 15035–15039, 2003

Printed in U.S.A.

Mapping the Collagen-binding Site in the von Willebrand Factor-A3 Domain*

Received for publication, September 3, 2002, and in revised form, January 22, 2003
Published, JBC Papers in Press, February 11, 2003, DOI 10.1074/jbc.M208977200

Roland A. Romijn‡, Erik Westein‡, Barend Bouma§¶, Marion E. Schiphorst‡, Jan J. Sixma‡, Peter J. Lenting‡, and Eric G. Huizinga‡§‖

From the ‡Thrombosis and Haemostasis Laboratory, Department of Haematology, University Medical Center and Institute of Biomembranes, HP G03.647, P. O. Box 85500, 3508 GA Utrecht, The Netherlands and §Bijvoet Center for Biomolecular Research, Department of Crystal and Structural Chemistry, Utrecht University, Padualaan 8, 3584 CH Utrecht, The Netherlands

The multimeric glycoprotein von Willebrand factor (VWF) mediates platelet adhesion to collagen at sites of vascular damage. The binding site for collagen types I and III is located in the VWF-A3 domain. Recently, we showed that His^{1023}, located near the edge between the "front" and "bottom" faces of A3, is critical for collagen binding (Romijn, R. A., Bouma, B., Wuyster, W., Gros, P., Kroon, J., Sixma, J. J., and Huizinga, E. G. (2001) *J. Biol. Chem.* 276, 9985–9991). To map the binding site in detail, we introduced 22 point mutations in the front and bottom faces of A3. The mutants were expressed as multimeric VWF, and binding to collagen type III was evaluated in a solid-state binding assay and by surface plasmon resonance. Mutation of residues Asp^{979}, Ser^{1020}, and His^{1023} nearly abolished collagen binding, whereas mutation of residues Ile^{975}, Thr^{977}, Val^{997}, and Glu^{1001} reduced binding affinity about 10-fold. Together, these residues define a flat and rather hydrophobic collagen-binding site located at the front face of the A3 domain. The collagen-binding site of VWF-A3 is distinctly different from that of the homologous integrin α_2 I domain, which has a hydrophilic binding site located at the top face of the domain. Based on the surface characteristics of the collagen-binding site of A3, we propose that it interacts with collagen sequences containing positively charged and hydrophobic residues. Docking of a collagen triple helix on the binding site suggests a range of possible engagements and predicts that at most eight consecutive residues in a collagen triple helix interact with A3.

Under conditions of high shear stress, platelet adhesion to collagen at sites of vascular injury is initiated by the interaction of platelet receptor glycoprotein (Gp)[1] Ib-IX-V with collagen-bound von Willebrand factor (VWF) (1). Transient interactions between VWF and GpIb-IX-V mediate platelet rolling, which slows down the platelet and allows other platelet receptors such as integrin $\alpha_2\beta_1$ (2) and GpVI to bind to collagen (2–4). These interactions result in firm adhesion and activation of platelets at the site of vascular injury.

VWF is a multimeric glycoprotein consisting of ~270-kDa monomers that are linked by disulfide bonds (5). The affinity of VWF for collagen depends on multimer size (6). The binding site for fibrillar collagens type I and III is located in the VWF-A3 domain (7), whereas collagen type VI has been shown to bind to the VWF-A1 domain (8, 9). The latter domain also contains the binding site for GpIbα of the GpIb-IX-V complex (10, 11).

VWF A-type domains and homologous integrin I domains adopt a so-called dinucleotide-binding fold, or Rossman fold, composed of a central β-sheet flanked on both sides by amphipathic α-helices (12–15). Binding of the I domains of integrins $\alpha_1\beta_1$, $\alpha_2\beta_1$, $\alpha_{10}\beta_1$, and $\alpha_{11}\beta_1$ to collagen involves a divalent cation (16, 17) located in the metal ion-dependent adhesion site (MIDAS) motif, and amino acid residues at the top face of the domain (18, 19). Binding of the I domain of integrin $\alpha_2\beta_1$ to collagen induces a major displacement of its carboxyl-terminal α-helix that is thought to be critical for integrin signaling (18). The A3 domain of VWF does not contain a functional MIDAS motif, and binding of A3 to collagen is cation-independent (20, 21). The involvement of the top face of A3 in collagen binding has been excluded by mutagenesis studies (13, 22). Recently, we showed that His^{1023}, located close to the edge of the front and bottom face of A3, is critical for binding of VWF to collagen (23).

In this study, we identify the collagen-binding site in the VWF-A3 domain in detail by means of site-directed mutagenesis. We constructed 22 point mutants, expressed these as multimeric VWF, and evaluated their collagen binding characteristics.

EXPERIMENTAL PROCEDURES

Selection and Construction of VWF Point Mutants—Selection of amino acid residues for mutagenesis was based on the approximate location of the collagen-binding site as identified in our previous study (23) and the crystal structure of the VWF-A3 domain (12, 13). Selected residues are solvent-exposed in the isolated A3 domain. Residues Gln^{966}, Ser^{974}, Ile^{975}, Thr^{977}, Asp^{979}, Val^{980}, Pro^{981}, Asn^{983}, Val^{984}, Val^{985}, Ser^{993}, Val^{997}, Gln^{999}, Glu^{1001}, Gln^{1006}, Asp^{1009}, Ser^{1020}, Glu^{1021}, and Met^{1022} were mutated to alanine. In addition, Pro^{962}, Pro^{981}, and Pro^{1027} were mutated to histidine to inhibit collagen binding by steric hindrance. Backbone conformations of these proline residues suggested that the histidine side chain would protrude from the protein surface. Point mutations were introduced in the VWF-A3 domain using the QuikChange method (Stratagene, La Jolla, CA) as described previously (23).

Expression, Purification, and Characterization of VWF—VWF was

* This work was supported by the Council of Medical Science Program 902.26.193 from the Netherlands Organization for Scientific Research. The costs of publication of this article were defrayed in part by the payment of page charges. This article must therefore be hereby marked "*advertisement*" in accordance with 18 U.S.C. Section 1734 solely to indicate this fact.

¶ Present address: Laboratory of Medical Oncology, University Medical Center, HP F02.126, P. O. Box 85500, 3508 GA Utrecht, The Netherlands.

‖ To whom correspondence should be addressed. Tel.: 31-30-2533502; Fax: 31-30-2533940; E-mail: E.G.Huizinga@chem.uu.nl.

[1] The abbreviations used are: Gp, glycoprotein; MIDAS, metal ion-dependent adhesion site; SPR, surface plasmon resonance; VWF, von Willebrand factor; wt, wild-type.

stably expressed in baby hamster kidney cells overexpressing furin required for proper removal of VWF propeptide (7). Cells were cultured in serum-free medium. VWF was purified by immuno-affinity chromatography using monoclonal antibody RU8, which is directed against the D4 domain (7), and stored in 50 mM Hepes, 100 mM NaCl (pH 7.4) at −20 °C.

VWF concentration was determined by a sandwich enzyme-linked immunosorbent assay using polyclonal α-VWF and horseradish peroxidase-conjugated polyclonal α-VWF (DAKO, Glostrup, Denmark) for immobilization and detection, respectively (7). Normal pooled plasma from 40 healthy donors was used as a reference.

The multimeric structure of VWF was analyzed by agarose gel electrophoresis followed by Western blotting as described by Lawrie *et al.* (24).

Binding of monoclonal antibody RU5 (22) to VWF was analyzed as described previously (23), with some modifications. Microtiter plate wells (Costar, Cambridge, MA) were coated with a polyclonal antibody directed against the D′ and D3 domains of VWF (22) diluted to 2.5 μg/ml with 50 mM carbonate buffer (pH 9.6). Coating was carried out for 3 h at 37 °C. Wells were washed with PBS-T (phosphate-buffered saline containing 0.1% Tween 20) and blocked with 3% bovine serum albumin in PBS-T for 1 h at 37 °C. Expression medium containing VWF was diluted with mock medium to a final concentration of 1 μg/ml. Wells were incubated with diluted medium for 1 h at 37 °C. After washing, 2 μg/ml RU5 in PBS-T containing 3% bovine serum albumin was added for 1 h at 37 °C. Wells were washed again and incubated for 1 h at 37 °C with horseradish peroxidase-conjugated rabbit anti-mouse antibodies (DAKO) diluted 1:2500 in PBS-T containing 3% bovine serum albumin. *O*-Phenylenediamine was used as substrate for detection.

Static Collagen Binding Assay—Binding of VWF in expression medium to fibrillar human placenta collagen type III (catalogue no. C-4407; Sigma) was studied in a solid-state binding assay at a VWF concentration of 0.1 μg/ml as described previously (23).

Surface Plasmon Resonance Collagen Binding Assay—Surface plasmon resonance (SPR) binding studies were performed using a Biacore2000 system (Biacore AB, Uppsala, Sweden). Fibrillar collagen cannot be used in a Biacore system because it blocks the flow channels. Therefore, we used acid-soluble collagen type III. Previously, we have shown that binding of wt-VWF to acid-soluble collagen is similar to the binding of wt-VWF to fibrillar collagen in enzyme-linked immunosorbent assay (22). Human placenta collagen type III was dissolved in 50 mM acetic acid at a final concentration of 1 mg/ml (16 h, 4 °C) and immobilized on a CM5 biosensor chip using the amine coupling kit as instructed by the supplier. Approximately 3000 response units of collagen type III, which corresponds to 30 ng/mm^2, were immobilized. A reference channel was coated with a similar amount of human placenta collagen type IV (catalogue no. C-7521; Sigma) that does not interact with VWF (25). Analysis was performed in Biacore standard buffer containing 25 mM Hepes, 125 mM NaCl, 2.5 mM $CaCl_2$, and 0.005% (v/v) Tween 20 (pH 7.4) at 25 °C at a flow rate of 10 μl/min. Binding of VWF to the collagen type III-coated channel was corrected for nonspecific binding to the control channel (between 2% and 5%). VWF monomer concentrations were calculated on the basis of a monomer mass of 270 kDa. Collagen binding at equilibrium was determined at different VWF concentrations. To this end, increasing concentrations of VWF were injected. Each injection was continued for 30 min. The delay between injections was 7 min, during which time the biosensor chip was flushed with Biacore standard buffer. After measuring all concentrations of a VWF variant, the biosensor chip was regenerated by injection of 1 mM EDTA, 1 M NaCl, 0.1 M sodium citrate (pH 5.0) (1 min, 10 μl/min) and 10 mM taurodeoxycholic acid, 100 mM Tris (pH 9.0) (1 min, 10 μl/min), and 0.1 M H_3PO_4 (1 min, 10 μl/min).

Dissociation constants (K_D) and the number of binding sites expressed as the response at infinite VWF concentration ($R_{eq,max}$) were calculated as follows. First, the response at equilibrium (R_{eq}) was calculated for each association curve by fitting the data points with a 1:1 Langmuir interaction model (Biaeveluation software version 3.0.1). This interaction model fitted the experimental data well, despite the multivalent nature of the VWF-collagen interaction, with χ^2 values being typically lower than 1.5. Use of more complex binding models did not improve the fit significantly. Next, K_D and $R_{eq,max}$ were determined from the binding isotherms (R_{eq} plotted against VWF concentration) by fitting equation $R_{eq} = R_{eq,max}*[VWF]/(K_D + [VWF])$, which describes a 1:1 interaction. The fit was calculated using computer program GraphPad Prism (GraphPad Prism version 3.00 for Windows; GraphPad Software, San Diego, CA). Because interaction between VWF and collagen is multivalent and we used a 1:1 interaction model, calculated dissociation constants must be regarded as apparent values.

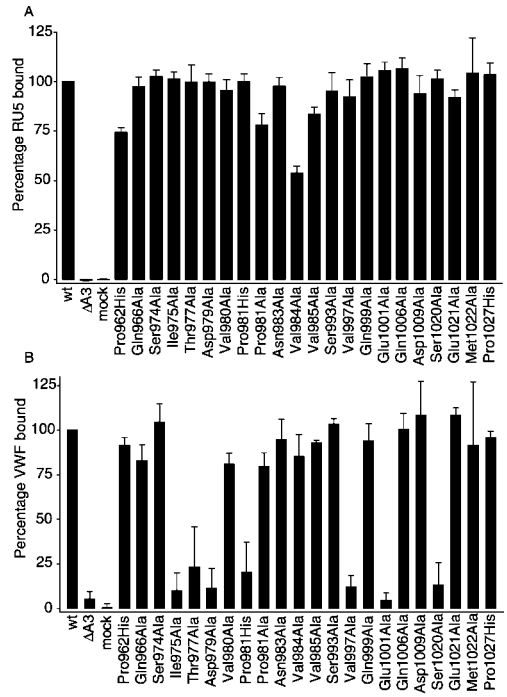

FIG. 1. **Characterization of VWF-A3 mutants.** *A*, binding of conformation-dependent antibody RU5. VWF was immobilized in microtiter plate wells via polyclonal antibody αD′D3. Immobilized VWF was incubated with RU5, and bound RU5 was detected as described under "Experimental Procedures." Wild-type VWF and ΔA3-VWF, which lacks the A3 domain (7), were used as a positive and negative control, respectively. Binding of RU5 to VWF mutants is expressed as a percentage of wt-VWF binding. Each *data point* represents the mean ± S.D. of three experiments performed in duplicate. *B*, binding of VWF point mutants to fibrillar collagen type III in a solid-state collagen binding assay. Human placenta collagen type III was coated in microtiter plate wells. Wells were incubated with VWF at a concentration of 0.1 μg/ml. Bound VWF was detected as described under "Experimental Procedures." ΔA3-VWF (7) was used as a negative control. Bound VWF is expressed as a percentage of wt-VWF binding. Each *data point* represents the mean ± S.D. of three independent experiments performed in duplicate.

RESULTS

Characterization of VWF Mutants—The conformation of the A3 domain and the multimeric size of VWF determine its reactivity toward collagen. Multimer distributions of VWF mutants and recombinant wt-VWF were indistinguishable (data not shown). The conformation of the A3 domain was evaluated with conformation-dependent monoclonal antibody RU5. Binding of RU5 to 18 of the 22 point mutants was similar to binding to wt-VWF. As expected, RU5 did not bind to ΔA3-VWF, a deletion mutant lacking the A3 domain (7) (Fig. 1*A*). Four of the point mutants, P962H, P981A, V984A, and V985A, showed a significantly reduced RU5 binding, ranging from 60% to 80% compared with wt-VWF. However, collagen binding of these mutants was normal (see below). Reduced RU5 binding can be explained by direct interactions of the mutated residues with RU5, as observed in the crystal structure of the A3·RU5 complex (23). Overall, these data suggest that the A3 domains of all VWF variants are correctly folded.

Collagen Binding Affinity of VWF Mutants—In a first screen, the effect of mutations on binding to collagen type III was assessed by a solid-state collagen binding assay (Fig. 1*B*). Immobilized collagen was incubated with expression medium containing 0.1 μg/ml VWF. Binding of ΔA3-VWF to collagen was only 8% compared with wt-VWF. Mutations I975A, T977A, D979A, P981H, V997A, E1001A, and S1020A strongly reduced collagen binding, showing a residual binding of less than 25%.

To further investigate the effect of the seven mutations,

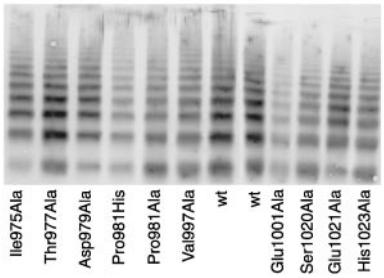

FIG. 2. **Multimer distributions of purified VWF variants.** The multimeric structure of purified VWF variants used in the SPR collagen binding assay was analyzed by agarose gel electrophoresis followed by Western blotting. The multimeric distributions of VWF mutants are similar to that of recombinant wt-VWF.

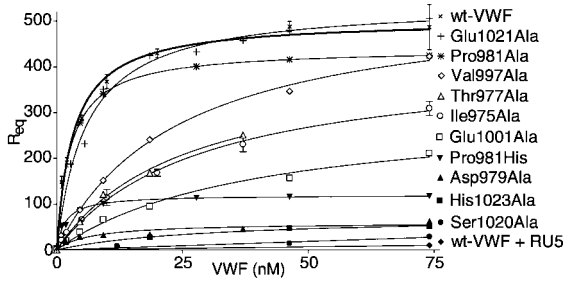

FIG. 3. **Binding isotherms of VWF mutants to collagen type III in an SPR-based assay.** Human placenta collagen types III and IV were immobilized on a CM5 biosensor chip for a detection and reference channel, respectively. Increasing concentrations of VWF were injected, and binding at equilibrium was determined. Wild-type VWF and wt-VWF preincubated with a 5-fold molar excess of RU5 Fab-fragment were used as a positive and negative control, respectively. Each variant was measured once, except for wt-VWF (×) and mutant I975A (○), which were measured four times using two independently purified batches of VWF and two sensor chips prepared with different batches of collagen. The *error bars* represent the S.D. calculated from these four measurements. Coefficients of variation determined from these multiple measurements are 10% and 25% for the dissociation constants and 1.9% and 4.3% for the maximum binding of wt-VWF and mutant I975A, respectively. Binding constants derived from the binding isotherms are listed in Table I.

these mutants and mutant H1023A from our previous study (23) were purified by immuno-affinity chromatography, and collagen binding was analyzed by SPR. We also purified and analyzed wt-VWF and mutants P981A and E1021A that bound normally to collagen in the solid-state collagen binding assay. The multimer distribution of the VWF variants after purification was similar (Fig. 2).

Addition of the RU5 Fab fragment to wt-VWF almost completely inhibited collagen binding, confirming that the A3 domain contains the binding site for collagen type III (Fig. 3). Mutants P981A and E1021A, which bound normally to collagen in the solid-state collagen binding assay, also had similar binding affinities and a similar number of binding sites as wt-VWF in the SPR-based collagen binding assay (Fig. 3). Mutants that exhibited strongly reduced collagen binding in the solid-state assay divided in two populations in the SPR collagen binding assay. Mutations I975A, T977A, V997A, and E1001A reduced the affinity of VWF for collagen 5–10-fold, whereas at saturation, the number of binding sites was at least 60% compared with wt-VWF (Table I). Mutants D979A, P981H, S1020A, and H1023A had a residual binding at saturation of less than 20% compared with wt-VWF.

As shown in Fig. 4*A*, mutations that reduce collagen binding are located at the front face of the domain and define a rather flat collagen-binding site. Mutations at the bottom face did not have an effect. Surface properties of the collagen-binding site are shown in Fig. 4, *B* and *C*. The upper part of the collagen-binding site contains a small negatively charged patch. In addition, the collagen-binding site contains one large hydrophobic patch and two smaller hydrophobic patches.

Docking of a Collagen Triple Helix on A3—The amino acid sequence of collagen that is recognized by the VWF-A3 domain is not known. Under these circumstances, the use of automated docking procedures, such as FTdock (26) and AutoDock (27), that use scoring functions based on shape complementarity and interaction energies is not meaningful. Therefore, we used the interactive molecular graphics program O (28) to obtain an impression of possible collagen-binding modes compatible with structural and mutagenesis data. Because the amino acids of A3 that are involved in collagen binding define an extended and rather flat surface at the front face of the domain, a bound collagen triple helix must lie nearly parallel to the front face. A model of a triple helix restricted to lie parallel to the front face of A3 was rotated and translated with respect to A3, and two criteria were evaluated to select possible binding modes. Firstly, the collagen triple helix should contact ($d < 4$ Å) all residues of A3 involved in collagen binding. Secondly, monoclonal antibody RU5 bound to A3, as observed in the crystal structure of the A3·RU5 complex (23), should block ($d < 2$ Å) binding of collagen by sterical hindrance. For the evaluation of distances, we assumed a fairly large radius for the collagen triple helix of 9 Å, which corresponds to the approximate distance from the tip of an extended lysine side chain to the center of the triple helix. Using a smaller radius would have reduced the range of possible binding modes, but in the absence of knowledge about the collagen residues actually involved, this did not seem justified.

A range of orientations of the collagen triple helix fulfilled the criteria (Fig. 4*D*). In these potential binding modes, the collagen triple helix lies at an angle of about 60° to 90° to strand β3 (located at the front face of the domain) and interacts with the A3 domain via six to eight consecutive residues.

TABLE I
Apparent dissociation constants and maximum binding for the VWF-collagen interaction

Binding constants were derived from the binding isotherms shown in Fig. 3.

VWF variant	$K_D \pm$ SE[a]	$R_{eq,max}$[b] $\pm$ SE[a]
	nM	*RU*
wt-VWF	3.3 ± 0.3	503 ± 10
P981A	2.7 ± 0.2	440 ± 8
E1021A	5.8 ± 0.6	540 ± 14
I975A	28 ± 2.8	420 ± 18
T977A	25 ± 4.4	419 ± 38
V997A	24 ± 2.5	551 ± 23
E1001A	39 ± 8.1	310 ± 31
D979A[c]		50
P981H	1.7 ± 0.2	120 ± 3.3
S1020A[c]		30
H1023A[c]		50

[a] S.E. of the fitted values from nonlinear regression.
[b] Maximum binding is expressed as the response at infinite VWF concentration.
[c] Collagen binding of these variants was too low to calculate reliable K_D values. $R_{eq,max}$ for these mutants was estimated from the binding isotherms at a VWF concentration of 74 nM.

DISCUSSION

Von Willebrand factor A-type domains are found in many proteins including collagens, complement proteins, and integrins, where they are named I domains. These proteins are involved in several biological functions such as cell-cell interaction and ligand-receptor binding. In integrins, these interactions involve a divalent cation present in the MIDAS motif located at the top of the domain.

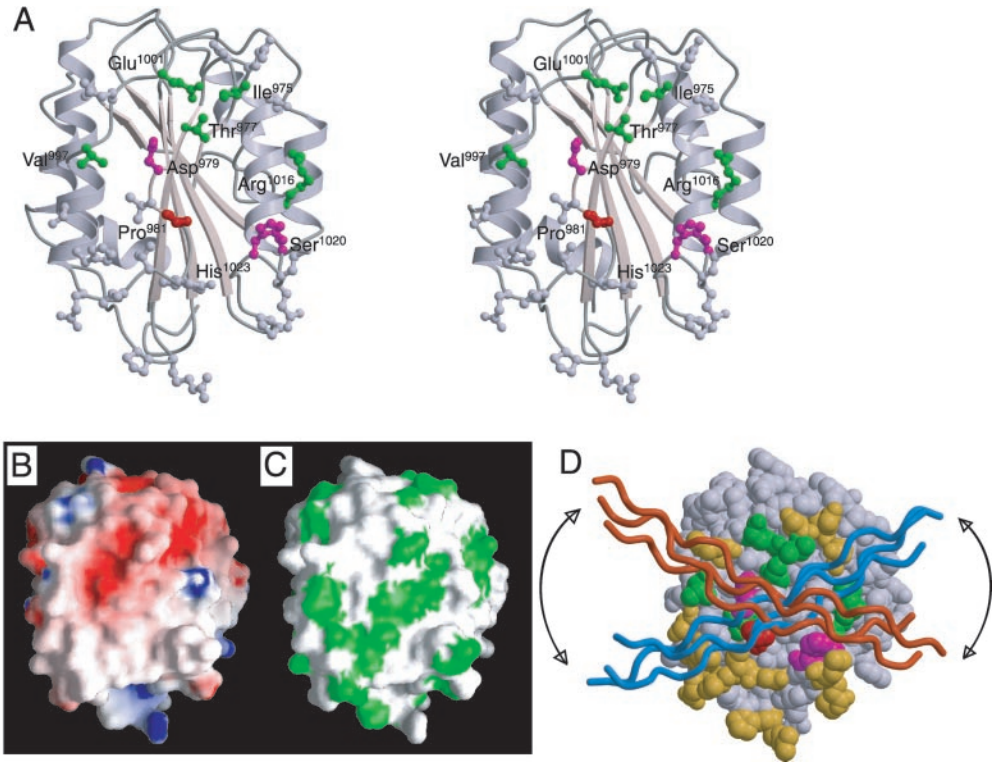

FIG. 4. **Characteristics of the collagen-binding site on the VWF-A3 domain.** *A*, stereoview of the A3 domain that shows the effect of mutations on collagen binding by color. Mutation of residues shown in *magenta* strongly reduces collagen binding. Mutation of residues shown in *green* partially reduces collagen binding, whereas mutation of residues shown in *gray* has no effect. Pro^{981} is shown in *red*. Mutation P981A has no effect on collagen binding, whereas mutation P981H strongly reduces binding. The effect of five mutations investigated in our previous study (23), R963A, E987A, H990A, R1016A, and H1023A, are included in the figure. *B*, solvent-accessible surface with electrostatic potential contoured from *red* (−260 mV) to *blue* (+260 mV). *C*, solvent-accessible surface with hydrophobic and hydrophilic regions in *green* and *white*, respectively. *D*, space-filling representation of the A3 domain with two collagen triple helices that indicate the putative range of orientations for the A3-collagen interaction. Residues of A3 are color-coded as described in *A*, except that residues that show no effect on collagen binding are colored *yellow*, and residues for which no data are available are shown in *gray*. Figures were generated with MOLSCRIPT (36), RASTER3D (37), and GRASP (38). The atomic coordinates for the crystal structure of A3 were taken from Protein Data Bank entry 1ATZ (12).

VWF contains three A-type domains, of which the A3 domain binds to collagen. The VWF-A3 domain does not contain a functional MIDAS motif, and collagen binding is cation-independent (20, 21). Previously, we excluded the top face of A3 from being involved in collagen binding (22) and showed that His^{1023}, located close to the edge of the front and bottom face, is critical for binding of VWF to collagen (23). Based on these results, we constructed a panel of 22 point mutants in which solvent-exposed residues were mutated to either alanine or histidine. These mutations were introduced in multimeric VWF, and the binding of these VWF mutants to collagen type III was evaluated.

In a solid-state collagen binding assay, 7 of the 22 mutants, namely, I975A, T977A, D979A, P981H, V997A, E1001A, and S1020A, displayed reduced collagen type III binding. None of these mutations are located at the bottom face of A3, excluding its involvement in collagen binding. We further characterized these seven mutants and mutant H1023A, which also displays strongly reduced collagen binding (23), by SPR. In contrast to the solid-state binding assay, SPR analysis measures collagen binding under equilibrium conditions and is not affected by washing steps. The apparent dissociation constant for binding of wt-VWF to collagen type III as determined by SPR was 3.3 nM, which is similar to values previously determined by us and others (22, 29). Interestingly, mutants that were qualified as "strongly reduced" in the solid-state assay separated in two groups in the SPR analysis. Mutants D979A, S1020A, and H1023A displayed a large reduction in affinity and in the number of binding sites, showing that these residues are critical for collagen type III binding. In contrast, mutants I975A, T977A, V997A, and E1001A were characterized by a 5–10-fold reduced affinity but had a near normal number of binding sites, indicating that these residues contribute to collagen binding but are not essential. Residues essential for collagen binding are located in strand $\beta 3$ and loop $\alpha 3\beta 4$ in the lower half of the front face of A3, whereas nonessential residues are located in the upper half of the front face in loops $\beta 2\beta 3$, $\alpha 2\alpha 3$, helix $\alpha 3$, and strand $\beta 3$ (Fig. 3*A*).

Mutation of Pro^{981} to alanine did not affect collagen binding, whereas mutation to histidine markedly decreased VWF binding to collagen. Apparently, Pro^{981} is not required for binding to collagen type III, but the introduction of a bulky histidine side chain at the lower half of the front face of the domain interferes with collagen binding via sterical hindrance. This observation further supports our conclusion that the collagen-binding site is located at the front face of A3.

Docking of a collagen triple helix on the front face of the A3 domain suggested a range of possible engagements (Fig. 4*D*) and predicts that at most eight consecutive residues in a collagen molecule interact with A3. Based on the surface characteristics of the collagen-binding site (Fig. 4, *B* and *C*), we propose that collagen sequences recognized by A3 contain positively charged and hydrophobic residues.

Despite their similarity in fold and ligand, VWF-A3 and collagen-binding integrin I domains have distinctly different binding sites. In A3, a rather hydrophobic and flat binding site is located at the front face, whereas integrin I domains bind collagen in a predominantly hydrophilic groove at their top face and require a functional MIDAS motif (18, 30). Integrin I domains undergo a large conformational change upon collagen

binding that makes them particularly suited for signal transduction and modulation of ligand binding affinity (18). In contrast, the VWF-A3 domain appears to function as an independent structural unit, and there is no evidence for modulation of its collagen binding affinity, nor does binding of A3 to collagen appear to affect the affinity of the VWF-A1 domain for platelet receptor GpIbα. Thus, the collagen-binding site of A3 merely performs an adhesive function, whereas binding sites of I domains are more sophisticated and also play a regulatory role (31).

Recently, we determined the crystal structure of the VWF-A1 domain in complex with an amino-terminal fragment of platelet receptor GpIbα (11). Like A3, the A1 domain does not contain a MIDAS motif. GpIbα binds to two distinct sites on A1. The larger of the two binding sites is located at the front face of A1 and consists of residues from strand β3, helix α3, and loop α3β4. Interestingly, the same structural elements contribute residues to the collagen-binding site of A3, suggesting that ligand-binding sites in A-type domains that lack a MIDAS motive may all be located in a similar position at the front face of the domain.

Genetic screening has identified four mutations, S968T, Q971H, I978T, and Q999R, that affect binding of VWF to collagen (32, 33). These mutations are located at or just below the front surface of the domain, and their effect on collagen binding is consistent with our mutagenesis data. Surprisingly, these mutations caused no (32) or only moderate (33) bleeding symptoms, which questioned the relevance of the A3 domain for immobilization of VWF to the vascular matrix (32). However, Wu *et al.* (34) recently showed that collagen binding by the A3 domain is relevant because an antibody blocking the VWF-A3-collagen interaction prevented the formation of platelet-rich thrombi and prolonged the skin bleeding time at high doses. Further investigations are required to reconcile these conflicting observations and to establish the physiological importance of VWF-A3 in platelet adhesion.

After submission of this manuscript, Nishida *et al.* (35) reported mapping of the collagen-binding site of the VWF-A3 domain using a novel NMR technique. Their findings with regard to the location of the binding site and the orientation of a bound collagen triple helix are in complete agreement with our results.

In summary, the binding site for collagen type III is located at the front face of the VWF-A3 domain. Residues in the lower half of the collagen-binding site are essential for collagen binding, whereas residues in the upper half contribute to binding but are not essential. We suggest that a collagen triple helix that interacts with A3 contains hydrophobic and positively charged residues. Further understanding of the VWF-collagen interaction requires the identification of specific collagen sequences involved in VWF binding.

REFERENCES

1. Savage, B., Saldívar, E., and Ruggeri, Z. M. (1996) *Cell* **84,** 289–297
2. Savage, B., Almus-Jacobs, F., and Ruggeri, Z. M. (1998) *Cell* **94,** 657–666
3. Goto, S., Tamura, N., Handa, S., Arai, M., Kodama, K., and Takayama, H. (2002) *Circulation* **106,** 266–272
4. Kehrel, B., Wierwille, S., Clemetson, K. J., Anders, O., Steiner, M., Knight, C. G., Farndale, R. W., Okuma, M., and Barnes, M. J. (1998) *Blood* **91,** 491–499
5. Sadler, J. E. (1998) *Annu. Rev. Biochem.* **67,** 395–424
6. Fischer, B. E., Kramer, G., Mitterer, A., Grillberger, L., Reiter, M., Mundt, W., Dorner, F., and Eibl, J. (1996) *Thromb. Res.* **84,** 55–66
7. Lankhof, H., van Hoeij, M., Schiphorst, M. E., Bracke, M., Wu, Y. P., Ijsseldijk, M. J., Vink, T., de Groot, P. G., and Sixma, J. J. (1996) *Thromb. Haemostasis* **75,** 950–958
8. Hoylaerts, M. F., Yamamoto, H., Nuyts, K., Vreys, I., Deckmyn, H., and Vermylen, J. (1997) *Biochem. J.* **324,** 185–191
9. Denis, C., Baruch, D., Kielty, C. M., Ajzenberg, N., Christophe, O., and Meyer, D. (1993) *Arterioscler. Thromb.* **13,** 398–406
10. Lankhof, H., Wu, Y. P., Vink, T., Schiphorst, M. E., Zerwes, H. G., de Groot, P. G., and Sixma, J. J. (1995) *Blood* **86,** 1035–1042
11. Huizinga, E. G., Tsuji, S., Romijn, R. A. P., Schiphorst, M. E., De Groot, Ph. G., Sixma, J. J., and Gros, P. (2002) *Science* **297,** 1176–1179
12. Huizinga, E. G., Van der Plas, R. M., Kroon, J., Sixma, J. J., and Gros, P. (1997) *Structure* **5,** 1147–1156
13. Bienkowska, J., Cruz, M. A., Atiemo, A., Handin, R. I., and Liddington, R. (1997) *J. Biol. Chem.* **272,** 25162–25167
14. Colombatti, A., Bonaldo, P., and Doliana, R. (1993) *Matrix* **13,** 297–306
15. Emsley, J., King, S. L., Bergelson, J. M., and Liddington, R. C. (1997) *J. Biol. Chem.* **272,** 28512–28517
16. Tuckwell, D. S., Calderwood, D. A., Green, L. J., and Humphries, M. J. (1995) *J. Cell Sci.* **108,** 1629–1637
17. Dickeson, S. K., Walsh, J. J., and Santoro, S. A. (1997) *J. Biol. Chem.* **272,** 7661–7668
18. Emsley, J., Knight, C. G., Farndale, R. W., Barnes, M. J., and Liddington, R. C. (2000) *Cell* **100,** 47–56
19. Tulla, M., Pentikainen, O. T., Viitasalo, T., Kapyla, J., Impola, U., Nykvist, P., Nissinen, L., Johnson, M. S., and Heino, J. (2001) *J. Biol. Chem.* **276,** 48206–48212
20. Pietu, G., Fressinaud, E., Girma, J. P., Nieuwenhuis, H. K., Rothschild, C., and Meyer, D. (1987) *J. Lab. Clin. Med.* **109,** 637–646
21. Bockenstedt, P. L., McDonagh, J., and Handin, R. I. (1986) *J. Clin. Invest.* **78,** 551–556
22. Van der Plas, R. M., Gomes, L., Marquart, J. A., Vink, T., Meijers, J. C. M., de Groot, Ph. G., Sixma, J. J., and Huizinga, E. G. (2000) *Thromb. Haemostasis* **84,** 1005–1011
23. Romijn, R. A., Bouma, B., Wuyster, W., Gros, P., Kroon, J., Sixma, J. J., and Huizinga, E. G. (2001) *J. Biol. Chem.* **276,** 9985–9991
24. Lawrie, A. S., Horser, M. J., and Savidge, G. F. (1990) *Thromb. Haemostasis* **59,** 369–373
25. Sixma, J. J., van Zanten, G. H., Huizinga, E. G., Van der Plas, R. M., Verkley, M., Wu, Y. P., Gros, P., and de Groot, P. G. (1997) *Thromb. Haemostasis* **78,** 434–438
26. Gabb, H. A., Jackson, R. M., and Sternberg, M. J. E. (1997) *J. Mol. Biol.* **272,** 106–120
27. Morris, G. M., Goodsell, D. S., Halliday, R. S., Huey, R., Hart, W. E., Belew, R. K., and Olson, A. J. (1998) *J. Comput. Chem.* **19,** 1639–1662
28. Jones, T. A., Zou, J. Y., Cowan, S. W., and Kjeldgaard, M. (1991) *Acta Crystallogr. Sect. A* **47,** 110–119
29. Saenko, E., Kannicht, C., Loster, K., Sarafanov, A., Khrenov, A., Kouiavskaia, D., Shima, M., Ananyeva, N., Schwinn, H., Gruber, G., and Josic, D. (2002) *Anal. Biochem.* **302,** 252–262
30. Smith, C., Estavillo, D., Emsley, J., Bankston, L. A., Liddington, R. C., and Cruz, M. A. (2000) *J. Biol. Chem.* **275,** 4205–4209
31. Dickeson, S. K., Mathis, N. L., Rahman, M., Bergelson, J. M., and Santoro, S. A. (1999) *J. Biol. Chem.* **274,** 32182–32191
32. Schneppenheim, R., Obser, T., Drewke, E., Grosse-Wieltsch, U., Oyen, F., Sutor, A. H., Wermes, C., and Budde, U. (2001) *Blood* **98,** (suppl.) 41a
33. Ribba, A. S., Loisel, I., Lavergne, J. M., Juhan-Vague, I., Obert, B., Cherel, G., Meyer, D., and Girma, J. P. (2001) *Thromb Haemostasis* **86,** 848–854
34. Wu, D., Vanhoorelbeke, K., Cauwenberghs, N., Meiring, M., Depraetere, H., Kotze, H. F., and Deckmyn, H. (2002) *Blood* **99,** 3623–3628
35. Nishida, N., Sumikawa, H., Sakakura, M., Shimba, N., Takahashi, H., Terasawa, H., Suzuki, E. I., and Shimada, I. (2003) *Nat. Struct. Biol.* **10,** 53–58
36. Kraulis, P. (1991) *J. Appl. Crystallogr.* **25,** 649–950
37. Merritt, E. A., and Bacon, D. J. (1997) *Methods Enzymol.* **277,** 505–524
38. Nicholls, A., Sharp, K. A., and Honig, B. (1993) *Biophys. J.* **64,** 166–170